

On Application of the Weak Galerkin Finite Element Method to a Two-Phase Model for Subsurface Flow

Victor Ginting¹ · Guang Lin² · Jianguo Liu³

Received: 5 September 2014 / Accepted: 24 March 2015 / Published online: 31 March 2015
© Springer Science+Business Media New York 2015

Abstract This paper presents studies on applying the novel weak Galerkin finite element method (WGFEM) to a two-phase model for subsurface flow, which couples the Darcy equation for pressure and a transport equation for saturation in a nonlinear manner. The coupled problem is solved in the framework of operator decomposition. Specifically, the Darcy equation is solved by the WGFEM, whereas the saturation is solved by a finite volume method. The numerical velocity obtained from solving the Darcy equation by the WGFEM is locally conservative and has continuous normal components across element interfaces. This ensures accuracy and robustness of the finite volume solver for the saturation equation. Numerical experiments on benchmarks demonstrate that the combined methods can handle very well two-phase flow problems in high-contrast heterogeneous porous media.

Keywords Darcy equation · Heterogeneity · Local conservation · Saturation · Two-phase flow · Weak Galerkin finite element methods

Mathematics Subject Classification 65M60 · 65N30 · 76S05 · 76T99

V. Ginting was partially supported by US National Science Foundation under Grant DMS-1016283. G. Lin would like to acknowledge support by the Applied Mathematics program of the US DOE Office of Advanced Scientific Computing Research and Pacific Northwest National Laboratory's Carbon Sequestration Initiative, which is part of the Laboratory Directed Research and Development Program. J. Liu was partially supported by US National Science Foundation under Grant DMS-1419077.

✉ Jianguo Liu
liu@math.colostate.edu

Victor Ginting
vginting@uwyo.edu

Guang Lin
guanglin@purdue.edu

¹ Department of Mathematics, University of Wyoming, Laramie, WY 82071, USA

² Department of Mathematics, School of Mechanical Engineering, Purdue University, West Lafayette, IN 47907, USA

³ Department of Mathematics, Colorado State University, Fort Collins, CO 80523-1874, USA

1 Introduction

Mathematically and computationally sophisticated simulators of subsurface flow are in demand to address some of the most pressing problems faced by society and posed to scientists. For example, as the increasing population places more demand on energy resources, the society seeks to extract oil held tightly in petroleum reservoirs by forcing water and/or other chemicals into injection wells and recovering oil from production wells. In this case, we may forecast initial “breakthrough” times of the mix of the injected water and oil at production wells in addition to forecasting subsequent fractions of the two-phase flow of oil and water. Accompanying to the growing consumption of fossil fuel energy is the increasing pressure of carbon emission on the climate. Measures are sought to mitigate effects of carbon emissions on climate by sequestering carbon dioxide CO₂ emissions from fossil fuel combustion. For CO₂ sequestration [14], as a CO₂ brine is forced into one or more injection wells, it is desired to forecast breakthrough times of the brine at monitoring wells, which could serve simultaneously to recover displaced oil. A more acute situation was demonstrated in the reactor breach caused by the recent earthquake and ensuing tsunami in Japan. This places a serious call for monitoring and remediation of subsurface radioactive contamination.

Developing sophisticated simulators applicable to the aforementioned real world problems involves complicated physical, mathematical and computational concepts and tools. Over the past decade or so, research attention has focused on conditioning simulator forecasts to data and, to a lesser extent, on characterizing the uncertainty in forecasts, usually with few data to inform flow simulator parameters. Typically, the commonly used governing principles fall in the realm of multiphase flow in porous media [7, 9–12, 16, 17], in which the subsurface flow and transport of multiple components are governed by coupled differential equations of different type: an elliptic equation for pressure and a sequence of hyperbolic equations for component concentrations. Further complication arises from the heterogeneous and multiscale nature presented in the permeability field. Reliable numerical simulators are desired to handle these physical features accurately and robustly.

Central to numerical simulations of multiphase flow is the Darcy’s law, which relates the gradient of a phase pressure to permeability and associated velocity [7, 12]. In practice, the pressure information is rarely needed in a direct way. Instead it is almost imperative that the velocity profiles are available for subsequent transport solvers. As a statement of momentum conservation, the Darcy’s law takes two different forms and hence there are two different categories of numerical methods for solving the Darcy’s equation.

The first form has two first-order partial differential equations: one for the pressure, the other for the velocity. Corresponding to this form is the classical mixed finite element method (MFEM) and its variants. A finite element pair (one for pressure and the other for velocity) need to satisfy the well-known inf-sup condition in order to be used in the MFEM. There are many such admissible choices. A mixed finite element scheme produces a numerical pressure and a numerical velocity simultaneously, even though the numerical pressure has rarely subsequent use. It is the numerical velocity that is more important physically and used in subsequent applications, e.g., transport simulations. The main advantage of the MFEM is that the numerical flux is locally conservative and has a continuous normal component across element interfaces. These two desired properties are crucial for the correctness of any follow-up transport solver that uses the generated numerical flux. An obvious disadvantage of the MFEM is that the resulting linear system is indefinite, and requires special solvers such as the Uzawa algorithm.

The second form is a second order elliptic PDE about the pressure. The corresponding finite element methods are the continuous Galerkin finite element method (CGFEM) and the discontinuous Galerkin finite element method (DGFEM). These FEMs solve for a numerical pressure first. Then the gradient of the numerical pressure is taken along with certain postprocessing to obtain a numerical velocity. The CGFEM usually has a small number of pressure unknowns and the resulting discrete system is symmetric positive definite, but its numerical flux is not locally conservative and the normal flux is not continuous across element interfaces. Nontrivial postprocessing procedures need to be established [8] to obtain a numerical flux having the two desired properties. The DGFEM uses discontinuous shape functions on elements and hence has great flexibility in handling complicated geometry, even though interior penalty terms have to be introduced to enforce weak continuity across element interfaces. The numerical flux obtained directly from a DG pressure is locally conservative but does not have a continuous normal component across element interfaces [22]. Postprocessing procedures need to be established [3] to obtain a numerical flux having the two desired properties. Two known drawbacks in the DGFEM are proliferation of unknowns and problem-dependent penalty factors.

The recently developed weak Galerkin finite element method (WGFEM) [26] is a novel type of methods that maintain the advantages of the existing finite element methods but overcome their disadvantages. WGFEM uses degrees of freedom in element interiors and on mesh skeleton to establish a new type of approximations to differential operators. When applied to the Darcy equation [19], the WGFEM solves for a numerical pressure that is defined both inside elements and on element interfaces. The numerical pressure is then used to generate a discrete weak gradient and then a numerical flux that is both locally conservative and normally continuous across element interfaces. Compared to the MFEM [19], the WGFEM has the same number of unknowns but results in a definite system that is much easier to solve. Compared to the DGFEM, the WGFEM has less unknowns and has no need for choosing penalty factors. It has been demonstrated in [18] that the WGFEM can handle heterogeneity and anisotropy in permeability very well. It produces a numerical flux that has the two properties desired for robust transport simulations.

In this paper, we apply the WGFEM to two-phase flow problems that couple the Darcy equation and a saturation transport equation in a nonlinear manner. Specifically, the Darcy equation will be solved by the WGFEM, whereas the saturation equation will be solved by a finite volume method. Numerical experiments on benchmarks will demonstrate that the WGFEM is a viable (actually better) alternative to the classical MFEM in terms of solving the Darcy equation.

The rest of this paper is organized as follows. Section 2 sets up a model problem for two-phase flow and outline our numerical algorithm that is based on operator splitting. Section 3 presents the weak Galerkin finite element method and elaborates on the lowest-order weak Galerkin method on two-dimensional rectangular meshes. Section 4 presents numerical results on two benchmark problems to demonstrate the practical usefulness of WGFEM. Section 5 concludes the paper with some remarks on future work.

2 A Model Problem for Two-Phase Flow and Its Solution Procedure

2.1 A Two-Phase Model

In this section, we focus on the flow and transport in a domain Ω with heterogeneous permeability, governed by an immiscible two-phase system with a wetting phase and a nonwetting

phase (denoted by w and o , respectively), for example, water and oil. For simplicity of presentation, capillary pressure and gravity are not included in the model. The Darcy’s law combined with a statement of conservation of mass are expressed as

$$\nabla \cdot \mathbf{u} = q, \quad \text{where } \mathbf{u} = -\lambda(S)k(\mathbf{x})\nabla p, \tag{2.1}$$

and

$$\frac{\partial S}{\partial t} + \nabla \cdot (f(S)\mathbf{u}) = q_w, \tag{2.2}$$

where \mathbf{u} is the Darcy velocity, S is the saturation of the wetting phase, and k is the permeability coefficient. The total mobility $\lambda(S)$ and the flux function $f(S)$ are respectively given by

$$\lambda(S) = \frac{k_{rw}(S)}{\mu_w} + \frac{k_{ro}(S)}{\mu_o}, \quad f(S) = \frac{k_{rw}(S)/\mu_w}{\lambda(S)}, \tag{2.3}$$

where $k_{r\alpha}$ ($\alpha = w, o$) is the relative permeability of the phase α .

2.2 Solution Procedure

The two-phase system governed by (2.1) and (2.2) is multiphysics and multiscale in nature. The three unknowns (p, \mathbf{u}, S) to be solved depend on one another, as shown in Eq. (2.3). The dynamics of these unknowns are different from each other in the sense that typically the pressure and velocity vary on a larger time scale, compared to the saturation. Moreover, the spatial profiles of these unknowns are strongly affected by the permeability, whose values can span several orders of magnitude.

One widely adopted approach in the reservoir simulation community for solving a two-phase system is to employ the implicit pressure explicit saturation (IMPES) scheme [2]. Mathematically, this is an operator decomposition technique with which the pressure equation (2.1) is decoupled from the saturation equation (2.2) by lagging one time step behind calculations of the total mobility. This allows for solving (2.1) implicitly that gives (p, \mathbf{u}). Then the velocity \mathbf{u} is used to solve the saturation equation (2.2) explicitly. The IMPES scheme is illustrated in Fig. 1.

A stable discretization of the saturation equation relies crucially on the numerical approximation of \mathbf{u} satisfying the local conservation property. To be specific, given $\mathbf{u}_h \approx \mathbf{u}$, it is desirable to have

$$\int_{\partial E} \mathbf{u}_h \cdot \mathbf{n} ds = \int_E q dE. \tag{2.4}$$

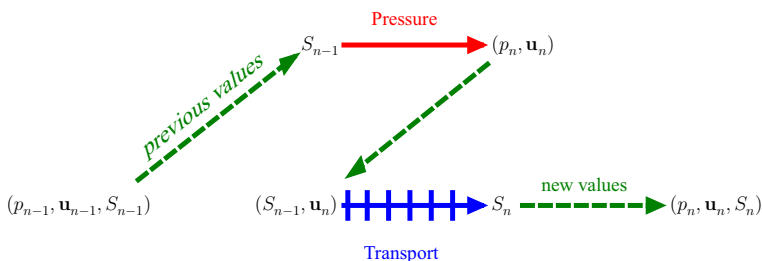


Fig. 1 A solution procedure for the two-phase flow model problem based on operator decomposition

In our setting, E is a finite element in a mesh for the domain Ω . A finite volume discretization of the saturation equation yields the following algebraic equations

$$|E|(S_{c,n} - S_{c,n-1}) + \Delta t \int_{\partial E} \mathbf{u}_h \cdot \mathbf{n} f(S_{c,n-1}) ds = \int_E q_w dE,$$

where

$$S_{c,n} \approx \frac{1}{|E|} \int_E S(x, t_n) dE$$

is the saturation average on element E at time t_n .

The explicit nature of the system is evident from the term $\int_{\partial E} \mathbf{u}_h \cdot \mathbf{n} f(S_{c,n-1}) ds$. In our numerical experiments, we use an upwinding scheme for this term [24].

3 Weak Galerkin Finite Element Method for the Darcy Equation

In this section, we present a weak Galerkin finite element scheme for solving the Darcy equation (2.1). This scheme furnishes a numerical velocity that is locally conservative and has continuous normal components across element interfaces. To present the idea, we consider

$$\begin{cases} \nabla \cdot (-\mathbf{K}\nabla p) = q & \text{in } \Omega \subset \mathbb{R}^2 \\ p = p_D & \text{on } \Gamma_D \\ (-\mathbf{K}\nabla p) \cdot \mathbf{n} = g_N & \text{on } \Gamma_N \end{cases} \tag{3.1}$$

with Dirichlet and Neumann boundary conditions given by p_D , g_N , respectively, and a forcing term q . Here $\mathbf{K} = \lambda k(\mathbf{x})$ and λ has been calculated from the saturation at the previous time step, see the algorithm illustrated Fig. 1.

As discussed in the Introduction, many finite element methods solve for the primal variable pressure first and then produce velocity and flux, e.g., the CGFEMs, DGFEMs, and the WGFEMs to be presented. All these finite element methods are based on the variational formulation

$$\int_{\Omega} \mathbf{K}\nabla p \cdot \nabla \phi = \int_{\Omega} q \phi. \tag{3.2}$$

Two common issues for CG, DG, WG are

- How will the gradient in (3.2) be approximated?
- Where are the degrees of freedom (DOFs) placed?

For CG, the DOFs are placed at mesh nodes and on edges and inside elements (depending on the order of the finite elements). Then the classical gradients of the polynomial shape functions are used to approximate the gradient in (3.2).

For DG, all DOFs are inside element interiors, the classical gradients of the polynomial shape functions are used along with penalty terms for approximation of the gradient in (3.2).

For WG, DOFs are placed in element interiors and on element interfaces. They are combined through integration by parts to produce discrete weak gradients, which are used to approximate the gradient in (3.2).

The weak Galerkin finite element method was first introduced in [26] based on a family of novel concepts such as weak functions, discrete weak functions, weak gradient, and discrete weak gradients. Generally speaking, the WGFEM provides a new framework that allows us to design new types of finite elements and use discrete weak gradients to approximate the classical gradient in (3.2).

For the WGFEM applied to (3.1), the introduction of pressure unknowns in element interior and on element interfaces offers both elementwise locality and connection among adjacent elements. This lays out the foundation for the local conservation and normal continuity of the numerical flux, which is computed using permeability and the discrete weak gradient of the numerical pressure.

3.1 Discrete Weak Gradients

Let E be a triangular or rectangular element with interior E° and boundary ∂E .

Let l, m be nonnegative integers, $P^l(E^\circ)$ be the space of polynomials on E° with degree $\leq l$, and $P^m(\partial E)$ be the space of polynomials on ∂E with degree $\leq m$. A **discrete weak function** is a pair of scale-valued functions $v = \{v^\circ, v^\partial\}$ such that $v^\circ \in P^l(E^\circ)$ and $v^\partial \in P^m(\partial E)$. A discrete weak function space on E is defined as

$$W(E, l, m) = \left\{ v = \{v^\circ, v^\partial\} : v^\circ \in P^l(E^\circ), v^\partial \in P^m(\partial E) \right\}. \tag{3.3}$$

Let $n \geq 0$ be any integer, $P^n(E)^2$ be the space of vector-valued polynomials with degree $\leq n$. Let $V(E, n)$ be a subspace of $P^n(E)^2$. For any $v \in W(E, l, m)$, its **discrete weak gradient** $\nabla_{w,d} v \in V(E, n)$ is so defined that it is the unique solution of

$$\int_E \nabla_{w,d} v \cdot \mathbf{w} dE = \int_{\partial E} v^\partial (\mathbf{w} \cdot \mathbf{n}) ds - \int_E v^\circ (\nabla \cdot \mathbf{w}) dE, \quad \forall \mathbf{w} \in V(E, n). \tag{3.4}$$

There could be many choices for $P^l(E^\circ)$, $P^m(\partial E)$, $V(E, n)$. But certain admissible conditions or properties shall be satisfied so that the discrete weak gradient operator $\nabla_{w,d}$ offers a Galerkin-type approximation of the classical gradient operator [26]. Furthermore, a projection operator $Q_h = (Q_h^\circ, Q_h^\partial)$ into a discrete weak function space can be defined, where Q_h° is the L^2 -projection into the polynomial space $P^l(E^\circ)$ and Q_h^∂ is the L^2 -projection into the polynomial space on $P^m(\partial E)$. Similarly, R_h is defined as the local (elementwise) L^2 projection from $L^2(E)^2$ to $V(E, n)$.

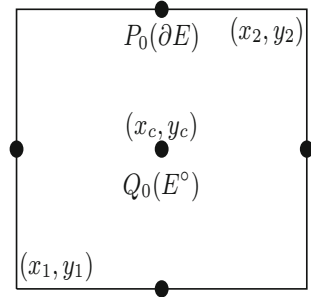
3.2 Weak Galerkin Elements $(Q_0, P_0, RT_{[0]})$ on Rectangular Meshes

As discussed in [18], there are a variety of choices for weak Galerkin (WG) finite elements that can be used for solving the Darcy equation. However, we concentrate on the lowest order WG elements for the Darcy equation in subsurface flow. This is mainly because the pressure solution usually possesses low regularity in this situation, and thus higher order WG finite elements do not result in additional gains. In this subsection, we further focus on the lowest order WG elements on rectangular meshes.

Let $E = [x_1, x_2] \times [y_1, y_2]$ be a typical rectangular element and (x_c, y_c) be its center. The divergence form of the Darcy equation (3.1) suggests that $V(E, n)$ should be chosen as $H(\text{div})$ -conforming. Therefore, the lowest order Raviart–Thomas space $RT_{[0]}(E)$ is undoubtedly a good candidate. It is known that $\dim(RT_{[0]}(E)) = 4$. We choose normalized basis functions [20] for $RT_{[0]}(E)$ as follows

$$\mathbf{w}_1 = \begin{bmatrix} 1 \\ 0 \end{bmatrix}, \quad \mathbf{w}_2 = \begin{bmatrix} 0 \\ 1 \end{bmatrix}, \quad \mathbf{w}_3 = \begin{bmatrix} X \\ 0 \end{bmatrix}, \quad \mathbf{w}_4 = \begin{bmatrix} 0 \\ Y \end{bmatrix},$$

Fig. 2 Five basis functions for a WG $(Q_0, P_0, RT_{[0]})$ rectangular element: one constant basis function in the interior of the rectangle and one constant basis function for each of the four edges. Their discrete weak gradients are defined in $RT_{[0]}$



where we have set $X = x - x_c, Y = y - y_c$ for convenience. An obvious advantage of using the normalized basis is that the Gram matrix is diagonal

$$GM = \text{diag} \left(|E|, |E|, \frac{1}{12}(x_2 - x_1)^2|E|, \frac{1}{12}(y_2 - y_1)^2|E| \right),$$

where $|E|$ is the area of the element. It is then trivial to invert the Gram matrix, which is needed for calculating the discrete weak gradients of the WG basis functions.

For WG basis functions, we choose $l = 0, m = 0$ respectively for $P^l(E^\circ), P^m(\partial E)$. So we have one constant basis function ϕ° in the element interior E° and one constant basis function $\phi_i^\partial (i = 1, 2, 3, 4)$ on each of the four edges (together forming ∂E) of the rectangle, as shown in Fig. 2. Their discrete weak gradients, actually the coefficients in the above $RT_{[0]}(E)$ basis functions, can be calculated by employing the definition formula (3.4). The results are as follows

$$\begin{cases} \nabla_{w,d}\phi^\circ = 0\mathbf{w}_1 + 0\mathbf{w}_2 + \frac{-12}{(x_2 - x_1)^2}\mathbf{w}_3 + \frac{-12}{(y_2 - y_1)^2}\mathbf{w}_4, \\ \nabla_{w,d}\phi_1^\partial = 0\mathbf{w}_1 + \frac{-1}{y_2 - y_1}\mathbf{w}_2 + 0\mathbf{w}_3 + \frac{6}{(y_2 - y_1)^2}\mathbf{w}_4, \\ \nabla_{w,d}\phi_2^\partial = \frac{1}{x_2 - x_1}\mathbf{w}_1 + 0\mathbf{w}_2 + \frac{6}{(x_2 - x_1)^2}\mathbf{w}_3 + 0\mathbf{w}_4, \\ \nabla_{w,d}\phi_3^\partial = 0\mathbf{w}_1 + \frac{1}{y_2 - y_1}\mathbf{w}_2 + 0\mathbf{w}_3 + \frac{6}{(y_2 - y_1)^2}\mathbf{w}_4, \\ \nabla_{w,d}\phi_4^\partial = \frac{-1}{x_2 - x_1}\mathbf{w}_1 + 0\mathbf{w}_2 + \frac{6}{(x_2 - x_1)^2}\mathbf{w}_3 + 0\mathbf{w}_4. \end{cases}$$

In summary, we have WG shape functions that are in Q_0 inside rectangular elements (interiors) and P_0 on edges (element interfaces) and their discrete weak gradients are in $RT_{[0]}$. This type of WG elements are referred as $(Q_0, P_0, RT_{[0]})$.

3.3 A Weak Galerkin Finite Element Scheme for the Darcy Equation

Let \mathcal{E}_h be a family of quasi-uniform rectangular meshes on a two-dimensional rectangular domain Ω . Let l, m be nonnegative integers. We define weak Galerkin finite element spaces on \mathcal{E}_h as follows

$$S_h(\mathcal{E}_h, l, m) = \left\{ v = \{v^\circ, v^\partial\} : v|_E \in W(E, l, m) \forall E \in \mathcal{E}_h \right\}, \tag{3.5}$$

$$S_h^0(\mathcal{E}_h, l, m) = \left\{ v = \{v^\circ, v^\partial\} \in S_h(l, m), v^\partial|_{\partial E \cap \Gamma_D} = 0 \forall E \in \mathcal{E}_h \right\}. \tag{3.6}$$

A weak Galerkin finite element scheme for (3.1) reads as: Seek $p_h = \{p_h^\circ, p_h^\partial\} \in S_h(\mathcal{E}_h, l, m)$ such that $p_h^\partial|_{\Gamma_D} = Q_h^\partial p_D$ and

$$\mathcal{A}_h(p_h, \phi) = \mathcal{F}_h(\phi), \quad \forall \phi = \{\phi^\circ, \phi^\partial\} \in S_h^0(\mathcal{E}_h, l, m), \tag{3.7}$$

where

$$\mathcal{A}_h(p_h, \phi) := \sum_{E \in \mathcal{E}_h} \int_E \mathbf{K} \nabla_{w,d} p_h \cdot \nabla_{w,d} \phi \, dE, \tag{3.8}$$

$$\mathcal{F}_h(\phi) := \sum_{E \in \mathcal{E}_h} \int_E q \phi^\circ \, dE - \sum_{\gamma \subset \Gamma_{N,h}} \int_\gamma g_N \phi^\partial \, ds. \tag{3.9}$$

After a numerical pressure p_h is obtained, one calculates its discrete weak gradient and then the numerical velocity as follows

$$\mathbf{u}_h = R_h(-\mathbf{K} \nabla_{w,d} p_h), \tag{3.10}$$

where R_h is the local L^2 projection onto $V(E, n)$ mentioned earlier. However, note that when $\mathbf{K} = K_E \mathbf{I}_2$ and K_E is a constant scalar on each element, the local L^2 projection in (3.10) is not needed. It is proved theoretically in [26] and demonstrated numerically in our recent work [18] that the WGFEM produces a numerical flux that is locally conservative elementwise as expressed in (2.4) and has continuous normal components across element interfaces.

A salient feature of the WG finite element scheme for the Darcy equation is that the discrete linear system is symmetric positive-definite, which can be solved by, e.g., the conjugate gradient method. This is an obvious advantage over the classical mixed finite element method, which results in indefinite linear systems and special solvers, e.g., the Uzawa algorithm, need to be used. WGFEM holds also advantages over the discontinuous Galerkin finite element method [19], which proliferates in number of unknowns and involves problem-dependent penalty factors.

3.4 Other Numerical Methods for the Darcy Equation

This subsection briefly discusses other related finite element methods for the Darcy equation (3.1), mainly the continuous Galerkin finite element method and the mixed finite element method.

3.4.1 CGFEM for Darcy

The CGFEM [4] is probably the simplest finite element method one can use for the Darcy equation (3.1). Here we briefly explain that the method does not produce a numerical velocity that is locally conservative and has normal components across element interfaces.

For simplicity, assume CG Q_1 elements are used on a rectangular mesh \mathcal{E}_h . Let $E \in \mathcal{E}_h$. Without loss of generality, assume the numerical pressure takes the form

$$p_h|_E = a + bx + cy + dxy.$$

Then one has a numerical velocity

$$\mathbf{u}_h = -K_E \begin{bmatrix} b + dy \\ c + dx \end{bmatrix}.$$

Assume K_E is a scalar constant on E , it is clear that

$$\nabla \cdot \mathbf{u}_h = 0.$$

So in general

$$\int_E q dE \neq 0 = \int_E (\nabla \cdot \mathbf{u}_h) dE = \int_{\partial E} \mathbf{u}_h \cdot \mathbf{n} ds,$$

Therefore, the local conservation property is not satisfied by the CG numerical velocity.

One can easily check the velocity values on two adjacent elements to find out that the normal component continuity property does not hold for the CG Q_1 finite element method.

A considerable amount of effort has been devoted to finding ways for postprocessing the approximate pressure of the CGFEM to produce a numerical velocity that is locally conservative and has continuous normal components across element interfaces [5, 8, 15]. Implementing the CG postprocessing procedure investigated in [8] takes also additional effort. There are difficulties in formulating the discrete system for the flux traces on the mesh skeleton, especially choosing a good base for the involved space of jumps.

Another remedy is to enhance the CG finite element space by piecewise constants [23].

3.4.2 MFEM for Darcy

The mixed finite element method has been widely accepted for solving the Darcy’s equation [18, 21]. It is based on the mixed formulation (the first form discussed in Introduction) of the Darcy’s law. A main advantage of the MFEM is that numerical flux and pressure are obtained simultaneously. Its main disadvantage is the need for indefinite discrete linear systems.

There are variants of the classical MFEM, e.g., hybridization of the MFEM [1, 6]. Contrary to the classical MFEM, the hybridized MFEM results in governing algebraic equations for the Lagrange multipliers or trace pressures, i.e., pressure values on the element interfaces. As a consequence, obtaining a velocity profile (as in the classical MFEM, it is still locally conservative) requires a postprocessing of the trace pressures.

The relationship between the MFEM, the hybridized MFEM, and the WGFEM is discussed in [18]. It has been demonstrated in [18, 19] that the numerical pressures, velocities obtained from using the WGFEM and the MFEM have negligible differences, when the permeability in the Darcy equation is a piecewise constant scalar.

4 Numerical Experiments

This section presents results of numerical experiments that examine the performance of the proposed methods. The main purpose is to accentuate robustness of the WGFEM in providing locally conservative velocity field. We measure this by checking the saturation profiles resulted from solving the transport equation by an upwinding finite volume scheme, for which the numerical velocity from the WGFEM is an input. A useful indicator is that the saturation profiles progressing over time should maintain its stability. This would otherwise be impossible, should the numerical velocity violate the local conservation.

In particular, we test two examples with distinct permeability fields shown in Figs. 3 and 6. Both examples of permeability exhibit high-contrast features, which can make solving (2.1) a demanding task. The ratio between the maximum and minimum values of $k(\mathbf{x})$ is related to the condition number of the resulting linear system for the finite element method for solving the Darcy equation.

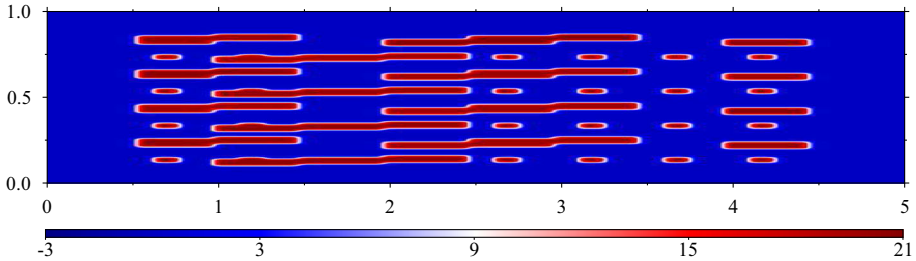


Fig. 3 Example 1: Logarithmic spatial profile of the permeability $k(\mathbf{x})$ exhibiting deterministic channel ($k_{\max}/k_{\min} \approx 3.966 \times 10^8$)

As mentioned earlier, the two-phase flow simulation is conducted using the operator decomposition procedure described in Sect. 2.1. A coarse scale time step Δt_c is used when dealing with the pressure equation (2.1), which is solved (implicitly) using the weak Galerkin finite element method. In other words, Eq. (2.1) is solved only for the coarse scale time levels. The time interval between two consecutive coarse time levels is divided into finer time levels using a fine scale time step Δt_f . Determination of Δt_f is controlled by the CFL condition, which needs to be satisfied to maintain stability of numerical solutions of first order hyperbolic equations. On these fine time levels, the saturation equation (2.2) is solved explicitly using an unwinding scheme. In this scheme, the velocity normal component is frozen at the previous coarse time level. The frozen normal component of numerical velocity is obtained from postprocessing of the weak Galerkin finite element solution at the aforementioned coarse time level.

We note that a standard unwinding scheme does require the input velocity normal component to the saturation equation (2.2) being locally conservative at a set of predefined control volumes. In this case, the said set of control volumes are the actual elements used for the discretization of the pressure equation (2.1) in the weak Galerkin finite element scheme, see (2.4) for the mathematical expression of local conservation.

For the physical parameters appearing in (2.1) and (2.2), we use the usual quadratic expressions for the constitutive relations: $k_{rw} = S^2$ and $k_{ro} = (1 - S)^2$ with two choices of viscosity ratio μ_o/μ_w : 5 and 20.

For both examples, the pressure boundary condition is set to 1 on the left boundary of Ω and 0 on the right boundary of the domain. The bottom and top boundaries of Ω are closed to flow at all times. No source or sink is present in the domain. The saturation boundary condition is set to 1 on the left boundary of Ω . The saturation at initial time is 0.

Example 1 The domain is $\Omega = [0, 5] \times [0, 1]$. The permeability field, as shown in Fig. 3, is posed on a 100×100 rectangular mesh. Here k_{\max}/k_{\min} is approximately 3.966×10^8 . Clearly, we have a high-contrast coefficient with abrupt transitions between regions of low and high permeability.

Within the framework of operator splitting, we use a coarse time step $\Delta t_c = 5 \times 10^{-3}$ and a fine time step $\Delta t_f = 10^{-4}$.

For the case the viscosity ratio $\mu_o/\mu_w = 5$, the saturation profiles at several time moments are shown in Fig. 4. It can be observed that the preferential transport of the water saturation is predominantly regulated by the high contrast feature of the permeability field. The saturation profiles in Fig. 4 shows that the saturation do not exceed 1 and are always nonnegative. This is an indication that the local conservation property is numerically represented. It would be

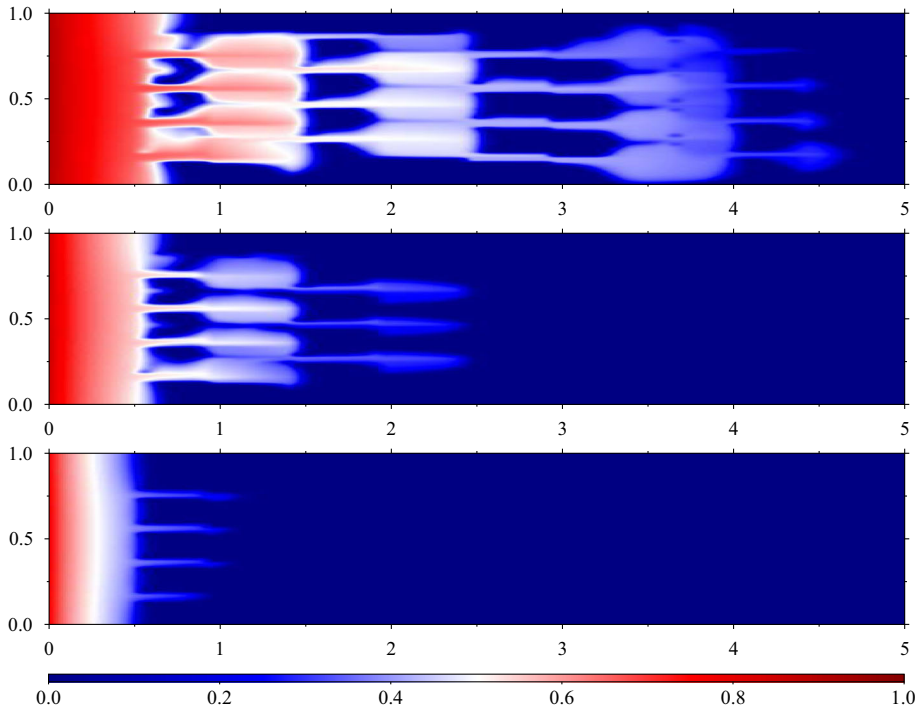
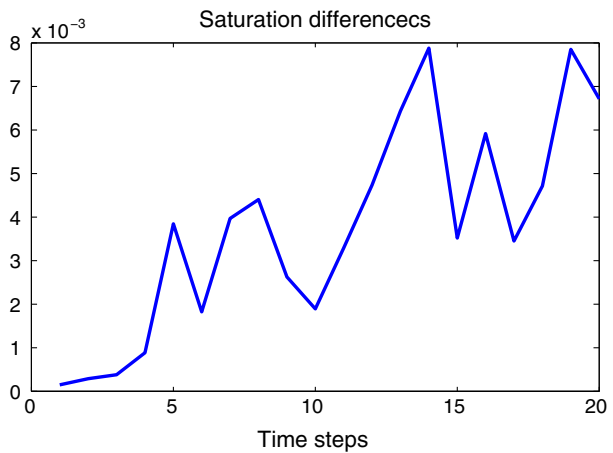


Fig. 4 Example 1: Saturation profiles obtained by using MGFEM+FVM: $t = 2.5$ (bottom), $t = 5$ (middle), and $t = 10$ (top). The viscosity ratio μ_o/μ_w is 5

Fig. 5 Example 1: Small differences in the saturations obtained by using WGFEM+FVM and MFEM+FVM at 20 coarse time steps



otherwise impossible to maintain, should the numerical velocity violate the local conservation property.

It was explained in [18] that there exists certain equivalence between the WGFEM and the MFEM when the permeability in the Darcy equation is a piecewise constant scalar. It has been demonstrated in [18,19] that the numerical pressures, velocities obtained from using the WGFEM and the MFEM have negligible differences. Here in this paper, for a

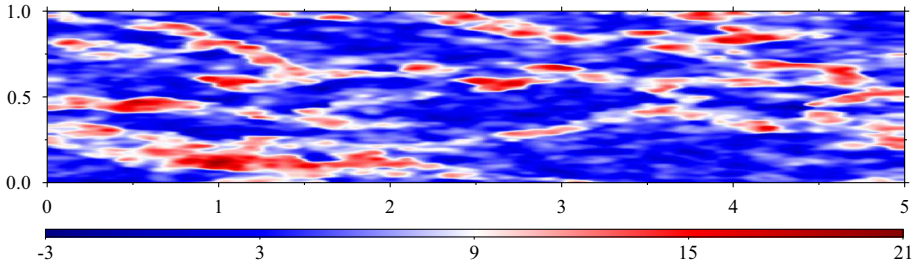


Fig. 6 Example 2: Logarithmic spatial profile of the permeability exhibiting random channel (with $k_{\max}/k_{\min} \approx 4.075 \times 10^9$)

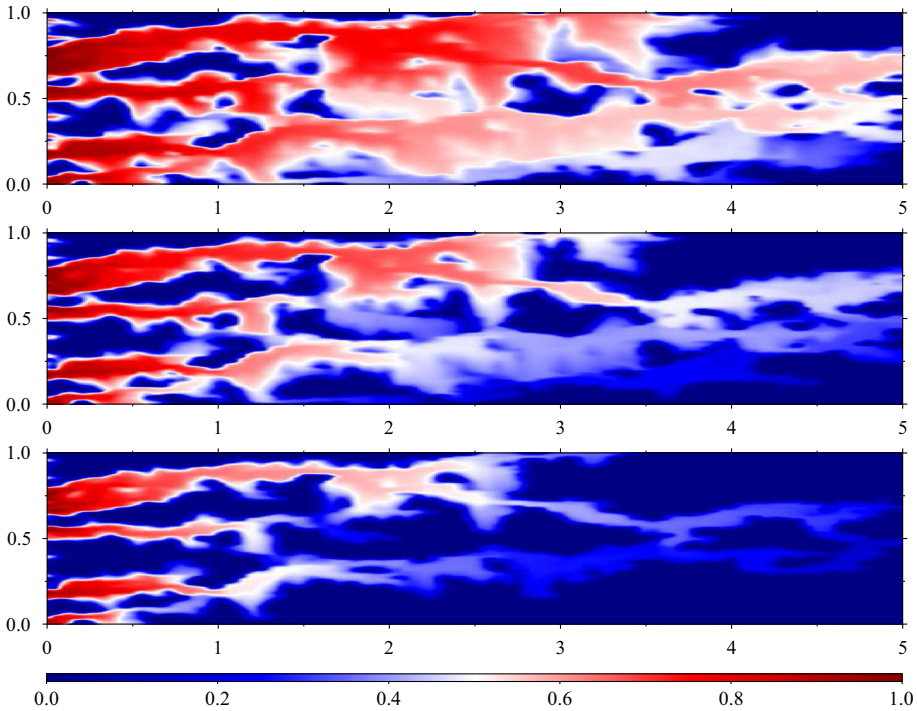


Fig. 7 Example 2: Saturation profiles with $k(\mathbf{x})$ using the randomly generated permeability: at $t = 0.025$ (bottom), $t = 0.05$ (middle), and $t = 0.1$ (top). The viscosity ratio μ_o/μ_w is 5

two-phase problem that couples the Darcy equation and a transport equation, we can observe similar phenomena. The two-phase problem (2.1)–(2.3) is solved respectively by WGFEM ($Q_0, P_0, RT_{[0]}$) for Darcy plus FVM for transport and MFEM ($RT_{[0]}, Q_0$) for Darcy plus FVM for transport. Note that the numerical fluxes obtained from solving (2.1) by WGFEM or MFEM are fed into the FVM solver for (2.2), which produces saturations. These saturations are fed into (2.3) to produce numerical permeabilities to be used in (2.1). Figure 5 shows the small differences between the saturation values for these two sets of numerical methods, even though the fluxes and saturations have been coupled nonlinearly in many steps of the numerical simulations. This evidence supports our statement that the WGFEM is a viable alternative of the MFEM for solving the Darcy equation.

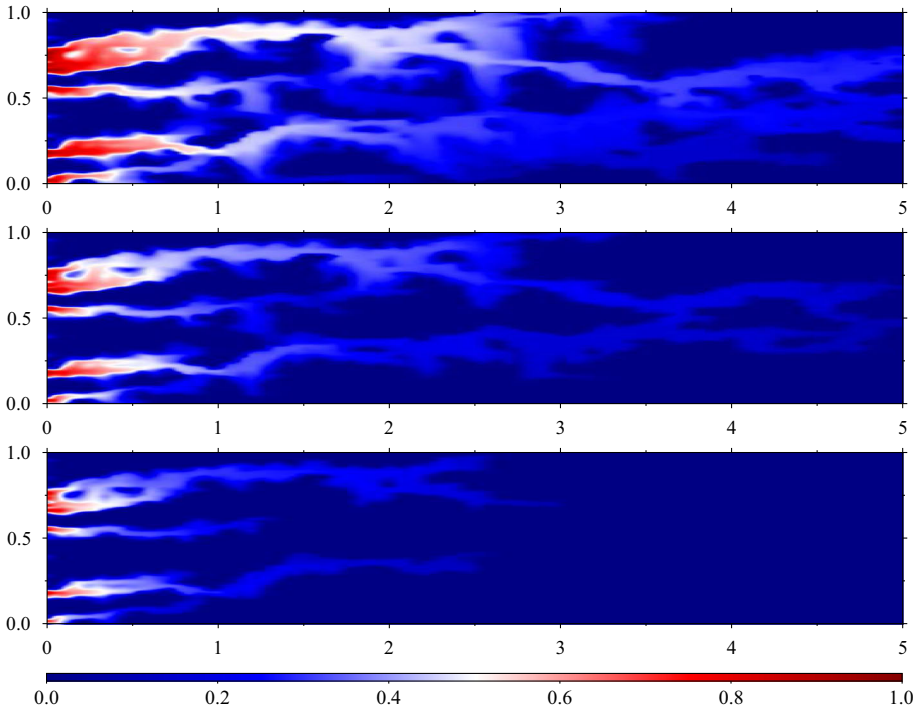


Fig. 8 Example 2: Saturation profiles with $k(\mathbf{x})$ using the randomly generated permeability: at $t = 0.025$ (bottom), $t = 0.05$ (middle), and $t = 0.1$ (top). The viscosity ratio μ_o/μ_w is 20

Example 2 The domain is still $\Omega = [0, 5] \times [0, 1]$, the permeability field is shown in Fig. 6. It is actually a single realization of a random, channelized permeability that is posed on a 120×120 rectangular mesh.

For the case the viscosity ratio $\mu_o/\mu_w = 5$, the saturation profiles sampled at several time moments are shown in Fig. 7. Here the coarse time step for flow is $\Delta t_c = 5 \times 10^{-5}$ whereas the fine time step for transport is $\Delta t_f = 10^{-6}$. As observed in the simulation results, the preferential transport is mainly governed by the channel feature of the permeability field albeit with irregular configuration.

For the case the viscosity ratio $\mu_o/\mu_w = 20$, Fig. 8 shows the saturation profiles at the same time moments.

Both figures exhibit the expected correct behavior in that the profiles maintain necessary stability. A slower transport is observed for the case of a viscosity ratio 20, compared to the case with a viscosity ratio 5.

These two test examples confirm the merit of a locally conservative flux with continuous normal component that is obtained from using the weak Galerkin finite element method.

5 Concluding Remarks

In this paper, we have combined the weak Galerkin finite element method and the finite volume method in numerical simulations of two-phase flow as typically found in subsurface

modeling. The weak Galerkin finite element method is utilized to solve the Darcy equation and has been demonstrated as accurately generating a locally conservative numerical velocity. This is crucial for robustness of the solver for saturation transport, particularly maintaining the positivity of saturation. The suitability of the combined methods has been substantiated by the simulation results on two benchmark test cases.

The study presented in this paper utilizes an upwinding finite volume method for solving the saturation transport equation. This method is subject to the restriction of the CFL condition. An alternative approach is to use characteristic finite volume methods [13], which allows us to use relatively large time steps. It is desirable to combine the weak Galerkin finite element methods with characteristic tracking [25] for development of transient convection-dominated transport equations. This is particularly important and useful for numerical simulations of multiphase flow when capillary pressure is included in the models. This is currently under our investigation and will be reported in our future work.

References

1. Arnold, D.N., Brezzi, F.: Mixed and nonconforming finite element methods: implementation, postprocessing and error estimates. *RAIRO Modél. Math. Anal. Numér.* **19**, 7–32 (1985)
2. Aziz, K., Settari, A.: *Petroleum Reservoir Simulation*. Applied Science Publishers, Barking (1979)
3. Bastian, P., Riviere, B.: Superconvergence and $h(\text{div})$ projection for discontinuous galerkin methods. *Int. J. Numer. Methods Fluids* **42**, 1043–1057 (2003)
4. Brenner, S.C., Scott, L.R.: *The Mathematical Theory of Finite Element Methods*. Texts in Applied Mathematics, vol. 15, 3rd edn. Springer, New York (2008)
5. Bush, L., Ginting, V.: On the application of the continuous galerkin finite element method for conservation problems. *SIAM J. Sci. Comput.* **35**, A2953–A2975 (2013)
6. Chavent, G., Roberts, J.: A unified physical presentation of mixed, mixed-hybrid finite elements and standard finite difference approximations for the determination of velocities in waterflow problems. *Adv. Water Resour.* **14**, 329–348 (1991)
7. Chen, Z., Huan, G., Ma, Y.: *Computational methods for multiphase flows in porous media*. SIAM, Philadelphia (2006)
8. Cockburn, B., Gopalakrishnan, J., Wang, H.: Locally conservative fluxes for the continuous galerkin method. *SIAM J. Numer. Anal.* **45**, 1742–1776 (2007)
9. Du, C., Liang, D.: An efficient S-DDM iterative approach for compressible contamination fluid flows in porous media. *J. Comput. Phys.* **229**, 4501–4521 (2010)
10. Efendiev, Y., Galvis, J., Lazarov, R., Margenov, S., Ren, J.: Robust two-level domain decomposition preconditioners for high-contrast anisotropic flows in multiscale media. *Comput. Methods Appl. Math.* **12**, 415–436 (2012)
11. Epshteyn, Y., Riviere, B.: Analysis of hp discontinuous galerkin methods for incompressible two-phase flow. *J. Comput. Appl. Math.* **225**, 487–509 (2009)
12. Ewing, R.: *The mathematics of reservoir simulation*. SIAM, Philadelphia (1983)
13. Healy, R., Russell, T.: Solutions of the advection–dispersion equation in two dimensions by a finite volume Eulerian–Lagrangian localized adjoint method. *Adv. Water Resour.* **21**, 11–26 (1998)
14. Hou, Z., Engel, D., Lin, G., Fang, Y., Fang, Z.: An uncertainty quantification framework for studying the effect of spatial heterogeneity in reservoir permeability on CO₂ sequestration. *Math. Geosci.* **45**, 799–817 (2013)
15. Hughes, T.J.R., Engel, G., Mazzei, L., Larson, M.G.: The continuous Galerkin method is locally conservative. *J. Comput. Phys.* **163**, 467–488 (2000)
16. Iliev, O., Lazarov, R., Willems, J.: Variational multiscale finite element method for flows in highly porous media. *Multiscale Model. Simul.* **9**, 1350–1372 (2011)
17. Kou, J., Sun, S.: Analysis of a combined mixed finite element and discontinuous Galerkin method for incompressible two-phase flow in porous media. *Math. Methods Appl. Sci.* **37**, 962–982 (2014)
18. Lin, G., Liu, J., Mu, L., Ye, X.: Weak galerkin finite element methods for darcy flow: anisotropy and heterogeneity. *J. Comput. Phys.* **276**, 422–437 (2014)
19. Lin, G., Liu, J., Sadre-Marandi, F.: A comparative study on the weak Galerkin, discontinuous Galerkin, and mixed finite element methods. *J. Comput. Appl. Math.* **273**, 346–362 (2015)

20. Liu, J., Cali, R.: A note on the approximation properties of the locally divergence-free finite elements. *Int. J. Numer. Anal. Model.* **5**, 693–703 (2008)
21. Raviart P.-A., Thomas, J. M.: A mixed finite element method for 2nd order elliptic problems. In: *Mathematical Aspects of Finite Element Methods (Proc. Conf., Consiglio Naz. delle Ricerche (C.N.R.), Rome, 1975)*, Lecture Notes in Math., vol. 606, pp. 292–315. Springer, Berlin (1977)
22. Riviere, B.: *Discontinuous Galerkin methods for solving elliptic and parabolic equations: theory and implementation*. SIAM, Philadelphia (2008)
23. Sun, S., Liu, J.: A locally conservative finite element method based on piecewise constant enrichment of the continuous galerkin method. *SIAM J. Sci. Comput.* **31**, 2528–2548 (2009)
24. Thomas, J. W.: *Numerical Partial Differential Equations, Vol. 33 of Texts in Applied Mathematics*. Springer, New York (1999). Conservation laws and elliptic equations
25. Wang, H., Liang, D., Ewing, R., Lyons, S., Qin, G.: An approximation to miscible fluid flows in porous media with point sources and sinks by an Eulerian–Lagrangian localized adjoint method and mixed finite element methods. *SIAM J. Sci. Comput.* **22**, 561–581 (2000)
26. Wang, J., Ye, X.: A weak galerkin finite element method for second order elliptic problems. *J. Comput. Appl. Math.* **241**, 103–115 (2013)